STAR Note 170
April 1994

SDD Signal Parametrization

(Preliminary results)

V. L. Rykov, R. Bellwied, A. French, J. R. Hall,
C. Pruneau, W. K. Wilson

Department of Physics and Astronomy
Wayne State University
Detroit, MI 48201

The primary goal of this study was to obtain a parametrization of silicon drift detector signals for the development of zero-suppresion algorithms for the Silicon Vertex Tracker data acquisition.

As it follows from the numerical simulations [1], an initial string-like ionization in a Silicon Drift Detector (SDD) [2] produced by a charged particle crossing the SDD plane transforms into a two-dimensional electron cloud with a gaussian-like shape. The width of the cloud $\sigma(t)$ is a monotonically increasing function of time and, in the case of perpendicular crossing, is expected to be the same in both the drift and transverse directions. The spatial charge density $\frac{d^2q}{dx\,dy}$ may be parametrized by the following:

$$\frac{d^2q}{dx\,dy} = \frac{Q_0}{2\pi\,\sigma^2(t)} \cdot \exp(-\frac{(x-x_c)^2+(y-y_c)^2}{2\sigma^2(t)}), \tag{1}$$

where Q_0 is a total electric charge; in this paper y is a distance measured from the anode along the drift direction and x is a distance measured in the transverse direction; (x_c, y_c) are the coordinates of the center of the cloud; x_c is not expected to change with drift time, whereas y_c is a linear function of time.

The primary ionized charge Q_0 may undergo partial recombination with time, even without stuctural inhomogeneities. However, in the present analysis we will not address this problem because of the lack of experimental data.

If we neglect Coulomb repulsion, the time-dependence of the width of the cloud has the following expression:

$$\sigma(t) = \sqrt{2Dt} \tag{2}$$

with a diffusion constant D of $\sim 3.0 - 3.5\,\mu m^2/ns$ at a temperature around $300\,^oK$ [3, 4].

Coulomb repulsion increases the cloud size and, in general, changes the time-dependence of $\sigma(t)$. However, for minimum ionizing particles ($Q_0 \leq 2 \cdot 10^4$) the contribution is not so large, and function (2) with D slightly above $3.5\,\mu m^2/ns$ fits the σ time-dependence with an accuracy of about 10% [5].

During the Fall-Winter 1993, SDD signal studies have been carried out at WSU (A. French, J. Hall) and LBL (C. Naudet, H. Rudolph). In the following, some early results from the data analysis are presented.

1 Measured values and their representations.

Experimental studies at WSU and LBL were performed with laser light substituting for charged particles. A primary local ionization in the SDD was created by a laser pulse of a few nanoseconds ($\sim 8\,ns$ in the WSU measurements). WSU used a laser diode which only forms a local ionization close to the surface, whereas the LBL laser penetrates the full wafer thikness of $300\,\mu m$. Shortly after its generation, the electron cloud is forced from the surface to the middle of the wafer and stays confined there to a thickness in z dimension around $5\,\mu m$. After drift along the SDD (in our notation "y-axis") the cloud arrives at the anodes ($240\,\mu m$ wide) which are located along the "x-axis" with a $10\,\mu m$ spacing between them. The anode signals were amplified and shaped and then directed to either a digital oscilloscope (at WSU) or a modified NA35 Switch Capacitor Array (SCA) (at LBL).

Due to the nonzero spatial size and time duration of the laser hit, an electron cloud initially has nonzero size in the (x, y)-plane and, in general, is anisotropic. Therefore, expression (1) has to be slightly modified. If the laser pulse shape in time and space is close to gaussian, for $t \gg t_{pulse}$, where t_{pulse} is the laser pulse time duration, the electron cloud shape may be described as

$$\frac{d^2q}{dx\,dy} = \frac{Q_0}{2\pi\,\sigma_x(t)\,\sigma_y(t)} \cdot \exp(-\frac{(x-x_c)^2}{2\sigma_x^2(t)} - \frac{(y-y_c)^2}{2\sigma_y^2(t)}) \tag{3}$$

For low primary ionization σ_x and σ_y may be approximated by:

$$\sigma_{x,y}(t) = \sqrt{\sigma_{0x,y}^2 + 2Dt}, \tag{4}$$

where the two constants σ_{0x} and σ_{0y} depend on the laser pulse parameters. The effective diffusion constant D is still expected to be the same, as in (2).

The distribution (3) can be rewritten in a similar form if, instead of the space coordinate "y" in the drift direction, we use the arrival time t of the electrons at the anodes:

$$\frac{d^2q}{dx\,dt} \simeq \frac{Q_0}{2\pi\,\sigma_x(t_c)\,\sigma_t(t_c)} \cdot \exp(-\frac{(x-x_c)^2}{2\sigma_x^2(t_c)} - \frac{(t-t_c)^2}{2\sigma_t^2(t_c)}), \tag{5}$$

where t_c is the arrival time of the cloud's "center of gravity". The time width $\sigma_t(t_c) \simeq \sigma_y(t_c)/V$ may be expressed by a formula similar to (4):

$$\sigma_t(t_c) = \sqrt{\sigma_{0t}^2 + 2Dt_c/V^2}, \tag{6}$$

where V is the drift velocity.

The time-dependence of the charge arriving at a given anode ($x = 0$ corresponds to the anode center), can be calculated with:

$$\frac{dq}{dt} \simeq \frac{Q_0}{2\pi\,\sigma_x(t_c)\,\sigma_t(t_c)} \cdot \exp(-\frac{(t-t_c)^2}{2\sigma_t^2(t_c)}) \cdot \int_{-d/2}^{d/2} dx \cdot \exp(-\frac{(x-x_c)^2}{2\sigma_x^2(t_c)}) \tag{7}$$

Here $d = 250\,\mu m$ is the width of the region along the x-axis, read out by a single anode.

The signal $A(t)$ measured at the amplifier-shaper (PASA) output corresponds to the input signal folded with the response function $f(t)$ of the electronics chain, which is the amplifier-shaper's response to the δ-function $\delta(t)$ at its input:

$$A(t) = \int_{-\infty}^{t} dt' \cdot \frac{dq(t')}{dt'} \cdot f(t-t') \; . \tag{8}$$

For an arbitrary $f(t)$, the time-dependence of $A(t)$ is not a gaussian any more. In the WSU measurements, the function $f(t)$ can be approximated by a triangle function, i. e.

$$f(t) \propto 1 - \frac{\mid t - t_f \mid}{\tau_f} \tag{9}$$

when $\mid t - t_f \mid \leq \tau_f$ with $\tau_f \simeq 85\,ns$ and $f(t) \simeq 0$ outside this interval. In this case the signal time width defined as

$$\sigma_t = \sqrt{< t^2 > - < t >^2} \tag{10}$$

still may be described by formula (6) with an accuracy of about 5%. The amplifier-shaper contribution to the σ_{0t}^2 is $\tau_f^2/6 \simeq (35\,ns)^2$. The moments $< t >$ and $< t^2 >$ are defined as:

$$< t^n > = (\int_{-\infty}^{\infty} t^n A(t) dt) / (\int_{-\infty}^{\infty} A(t) dt) \tag{11}$$

Below we list explicitly the parameters analyzed along with their analytic representations.

The centroid position $t_c(y)$**.** In this analysis the signal centroid $t_c = < t >$ was obtained by fitting gaussians $A_0 \cdot \exp(-\frac{(t-t_c)^2}{2\sigma_t^2})$ to the measured signal $A(t,x,y))$ with free parameters A_0, t_c and σ_t. Then, assuming the drift velocity V is a constant, the $t_c(y)$ dependence has been fitted with the linear function:

$$t_c(y) = t_0 + y/V, \tag{12}$$

with free parameters t_0 and V.

Time width $\sigma_t(y)$ has been fitted with the function:

$$\sigma_t(y) = \sqrt{\sigma_{0t}^2 + 2Dy/V^3} \tag{13}$$

with free parameters σ_{0t} and D. The value for the drift velocity V was taken from the fit (12).

Transverse width $\sigma_x(y)$ has been derived from the x-dependence of the amplitude $A_0(x,y)$ of the signal $A(t,x,y)$ at a fixed y and varied x. This dependence has been fitted with the function:

$$A_0(x,y) = P + \frac{C}{\sqrt{2\pi} \cdot \sigma_x(y)} \cdot \int_{-d/2}^{d/2} d\xi \cdot \exp(-\frac{(\xi - x - x_c)^2}{2\sigma_x^2(y)}) \tag{14}$$

with free parameters P, C, x_c and $\sigma_x(y)$ for $d = 250\,\mu m$. Then we attempted to fit the y-dependence of the σ_x with the function:

$$\sigma_x(y) = \sqrt{\sigma_{0x} + 2Dy/V} \tag{15}$$

with free parameters σ_{0x} and D.

2 Results.

All measurements from WSU presented here were performed on one specific wafer, SDD #395. The voltage U applied to the maximum drift distance of $L = 40\,mm$ was varied from 1500 to 2700 V.

2.1 Drift velocity and electron mobility.

The experimental results for the drift time $t_c(y)$ measurements along with the fits (12) are shown in Fig. 1. One can observe, that the $t_c(y)$ dependencies agree quite well with the expected linear function. However, at the highest voltage $U = 2700\,V$ (run "120693a") there is a significant nonlinearity at low y. The cause of this nonlinearity is under investigation. The electron mobility $m = V/E$, where $E = U/L$, derived from the different runs varies from 0.132 to 0.137 $\frac{mm^2}{V\cdot\mu s}$, i.e. within $\sim \pm 2\%$ (data from the run at "120693a" are not taken into account).

2.2 Time width σ_t.

The $\sigma_t(y)$ data from a number of WSU runs along with the fits (13)are presented in Fig. 2. Apparently, in some runs, irregularities like sudden drops, changing of the slopes, increasing the dispersion of experimental points, etc. were observed. The reason for such a behaviour is under investigation.

The fits to the data provide quite stable results for the σ_{0t}, in the range $35.3 - 37.7\,ns$, which corresponds to the expectations, that the main contribution of $\sim 35\,ns$ to the σ_{0t} is due to the amplifier-shaper.

Estimates for the diffusion constant, derived from the same runs, vary from 3.4 to $9.9\,\mu m^2/ns$. If we exclude the runs with visible irregularities, the measured $D \approx 7.5\,\mu m^2/ns$ is about twice as large as expected ($3.5 - 4\,\mu m^2/ns$ [3, 4]), assuming there is no Coulomb repulsion.

2.3 Transverse width σ_x.

The σ_x values at 7 fixed y positions were obtained from the fits using (14) for the measured x-dependencies of the amplitudes $A_0(x)$ (Fig. 4a-g) and "Areas" $= A_0(x) \cdot \sigma_t$ (Fig. 5a-g). The $\sigma_x(t_c)$ dependencies were then fitted with (15) treating σ_{0x} and D as free parameters. For the 3 points at the shortest distances y, a nonlinear dependence of the drift time on the drift distance has been observed (see Fig. 3 and compare it also with Fig. 1f), and it was taken in account in the fits shown in Figs. 6a, b. Figs. 6c, d represent the same data, but without this correction. Values for the diffusion constant D obtained from these fits are in the range of $4.2 - 4.7\,\mu m^2/ns$ which is close to expectations [3, 4]).

However, one can see, that function (15) does not fit the $\sigma_x(y)$ experimental points well, in particular at the small y. That might be due to the contribution of Coulomb repulsion, which, immediately after a local ionization is created, forces the electron cloud to expand more rapidly, i.e. provides the impression, that the effective diffusion constant is greater, than it actually is. This effect is getting smaller as the size of the electron cloud increases.

A simple way to improve a fit to experimental data is to represent the σ_x^2 time-dependence by a higher order polynomial function of t. For example, W. K. Wilson [7] uses in his simulation an expression: $\sigma = (a + bt_c)\sqrt{\sigma_0^2 + 2Dt_c}$, which is essentially identical to a higher order polynomial. Disadvantages of such an approximation are: first, there is no connection between parameters used and the physics of the phenomenon, and, second, this approximation has the wrong asymptotic behaviour at $t_c \to \infty$ which prevents its application outside the fitted t_c-interval.

To evaluate the $\sigma(t_c)$ behaviour for a small electron cloud (i.e. at low t_c), let us consider the following model for an electron cloud expansion with the zero size along z direction, and cylindrically symmetric in the (x, y) plane. The distribution function is:

$$\frac{d^2q}{dx\,dy} = Q_0 \cdot f(r,t), \tag{16}$$

where $r = \sqrt{x^2 + y^2}$, with a normalized $f(r,t)$:

$$2\pi \int_0^\infty f(r,t)\, r\, dr = 1.$$

Let us assume that, during the cloud expansion, its shape does not change, i.e.

$$f(r,t) = \frac{g(\frac{r}{\sigma(t)})}{\sigma^2(t)}. \tag{17}$$

The cloud width in either x or y directions is defined as:

$$\sigma^2(t) = \sigma_x^2(t) = \sigma_y^2(t) = \int_{-\infty}^{\infty} x^2\, dx \int_{-\infty}^{\infty} f(r,t)\, dy\ . \tag{18}$$

For $\sigma(t)$ evolution the following equation can be obtained (neglecting the effect of image charges):

$$\frac{d\sigma^2(t)}{dt} = 2D + \frac{Q_0 mK}{\sigma(t)}, \tag{19}$$

where D is the diffusion constant, m is the electron mobility. Assuming (17), coefficient K does not depend on t and can be calculated for the known $g(\frac{r}{\sigma(t)})$.

The solution of equation (19) is:

$$2Dt = \sigma^2 - \sigma_0^2 - \frac{Q_0 mK}{D}(\sigma - \sigma_0) + \frac{1}{2}(\frac{Q_0 mK}{D})^2 \ln(\frac{Q_0 mK + 2D\sigma}{Q_0 mK + 2D\sigma_0}), \tag{20}$$

where σ_0 is the initial width of the cloud at $t = 0$.

However, solution (20) is still too complicated and somewhat inconvenient for a fast SDD simulations,where a simple formula for $\sigma_x(t_c)$ is desirable. For example, we may consider the following expression:

$$\sigma(t_c) = \sqrt[3]{\sigma_0^3 + \frac{3}{2}Q_0 mK \cdot t_c + (2D \cdot t_c)^{3/2}}. \tag{21}$$

Although this is not a solution for the equation (19), it has the right asymptotic behaviour for $\frac{d\sigma^2}{dt_c}$ at $t_c \to \infty$ ($\frac{d\sigma^2}{dt_c} \to 2D$) as well as at low t_c where Coulomb repulsion dominates over diffusion ($\frac{d\sigma^2}{dt} \propto \sigma^{-1}$ when $t \to 0$).

Two-parameter fits (free parameters σ_0 and Q_0mK), employing (21), are shown in Fig. 6. The constant D was fixed, either to zero ("pure Coulomb"scenario) or to the expected value $3.5\,\mu m^2/ns$. Although the "pure Coulomb" gives a better fit than the other two approaches, the experimental uncertainties make it impossible to draw a firm conclusion about the relative contributions of Coulomb repulsion and diffusion at the present time. New measurements are currently in progress to reexamine the systematic errors.

In conclusion, for consistency, due to the presence of Coulomb repulsion, formula (13) for $\sigma_t(t_c)$ has also to be modified. One possible solution is:

$$\sigma_t(t_c) = \sqrt{\sigma_{a-s}^2 + \sqrt[3]{(\sigma_{0t}^3 + \frac{3}{2}Q_0mK \cdot t_c + (2D \cdot t_c)^{3/2})^2}}, \qquad (22)$$

where σ_{t0} is the initial size of an electron cloud and σ_{a-s} represents the contribution of the amplifier-shaper. However, based on the currently available experimental data for σ_t it seems problematic to get reliable information for all four parameters this function depends on.

3 Summary.

The centroid position $t_c(y)$ measurement showed quite stable results for the drift velocity and its dependence on the applied voltage. The measured electron mobility m varies within $\sim \pm 2\%$ and its experimental value is consistent with the expected $0.130 - 0.135\,mm^2/V \cdot \mu s$ at $\sim 300^o$K [3, 4].

Time width $\sigma_t(t_c)$ measurements provide reasonable results for the initial width $\sigma_{t0} \simeq 35\,ns$ and for the effective diffusion constant $D \simeq 7.5\,\mu m^2/ns$, if we take into account the probable significant contribution from Coulomb repulsion to the electron cloud expansion dynamics.

Transverse width $\sigma_x(t_c)$ measurements by scanning along the anodes, provide the most clean information about the electron cloud expansion dynamics, which are crucial to determine the real SVT features (position/momentum resolution, $\frac{dE}{dx}$ capabilities, etc). It is very desirable to get more measurements at different y and in the extended drift-time interval, which will be obtained by lowering the applied voltage.

In the future, it will be important to study parameter dependencies on the primary ionization level, covering the whole range, expected in the heavy ion collisions experiment. The simple expressions (21) and (22) and, in general, equation (19) and its solution (20) can be tested with numerical simulations of the electron cloud dynamics [1]. It is possible also to calculate the K factor in equation (19) and thus to obtain one more channel for the estimation of the primary ionization level during measurements.

In the short term, we plan to repeat some of the measurements described here, to obtain a more complete and consistent set of parameters for the SDD response function. To obtain analytical formulas for the electron cloud expansion dynamics suitable for the fast simulation, we are focusing our efforts on the better understanding of the effect of Coulomb repulsion. We are also going to measure the electron life-time in SDDs using recently assembled 90-channels data acquisition system based on VME.

References

[1] W. K. Wilson. STAR World Wide Web Documentation. "Resolution Simulator".

[2] E. Gatti and P. Rehak. NIM, **225**, 608 (1984)

[3] E. Gatti and P. F. Manfredi. Revista Nuovo Cimento, **9**, 1 (1986)

[4] W. C. Sailor, et al. NIM, **A303**, 285 (1991)

[5] W. K. Wilson. SDC Group Internal Report, January 4, 1994.

[6] H. Rudolph. Private communication.

[7] W. K. Wilson. Status of the SVT Resolution Simulator, September 4, 1992.

Figure Captions

Fig. 1. Drift time $t_c(y)$. SDD #395, L = 40 mm. WSU.

a) Run "100393a", U = 1500 V, anode #40. 10/03/93.

b) Run "092793c", U = 1500 V, anode #35. 09/27/93.

c) Run "100393d", U = 1500 V, anode #43. 10/03/93.

d) Run "092793e", U = 2000 V, anode #40. 09/27/93.

e) Run "092993a", U = 2000 V, anode #30. 09/29/93.

f) Run "120693a", U = 2700 V, anode #40. 12/06/93.

Fig. 2 Signal time-width $\sigma_t(y)$. SDD #395, L = 40 mm. WSU.

a) – f) the same runs as in Fig. 1

Fig. 3 Runs "3c20a" – "3c20g" (lateral scans). Drift time $t_c(y)$. SDD #395, L = 40 mm, U =2700 V, anode #40. WSU, December, 1993.

Fig. 4 Lateral scans along the x axis. Runs "3c20a" – "3c20g", SDD #395, L = 40 mm, U = 2700 V, anode #40. WSU, December, 1993: x-dependencies for the amplitude $A_0(x,y)$ at fixed y.

Fig. 5 Lateral scans along the x axis. Runs "3c20a" – "3c20g", SDD #395, L = 40 mm, U = 2700 V, anode #40. WSU, December, 1993: x-dependencies for the "Area" $Q(x,y) = A_0(x,y) \cdot \sigma_t(y)$ at fixed y.

Fig. 6 Time-dependencies of the transverse width $\sigma_x(t_c)$, derived (a, c) from the data in Fig. 4 for the amplitude, and (b, d) for the charge ("Area") – from the data in Fig. 5. Data in Fig. 7a, b are corrected, taking in account nonlinear $t_c(y)$ dependence (see Fig. 3).

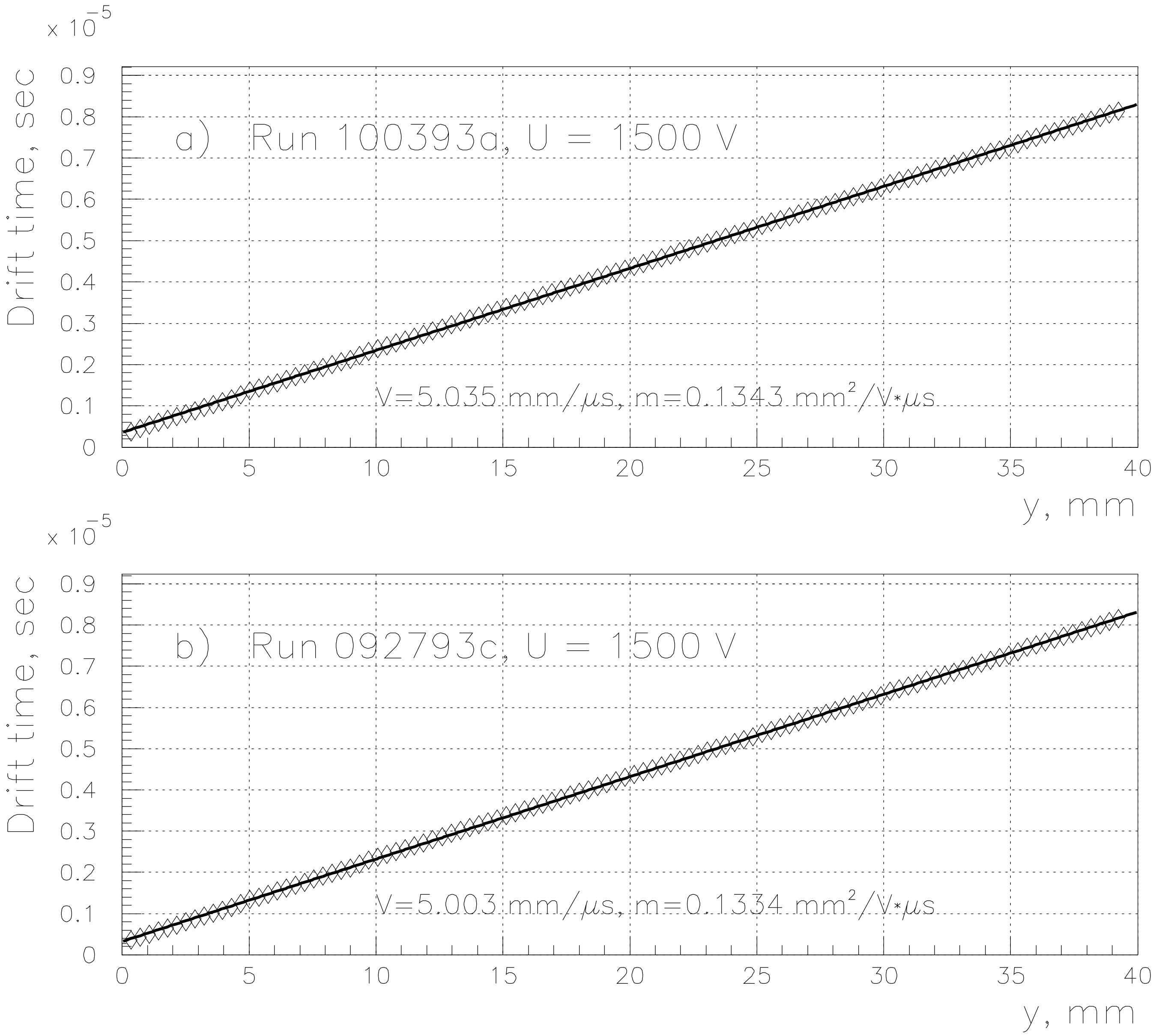
x 10^-5
Drift time, sec
a) Run 100393a, U = 1500 V
V=5.035 mm/μs, m=0.1343 mm²/V*μs
y, mm
x 10^-5
Drift time, sec
b) Run 092793c, U = 1500 V
V=5.003 mm/μs, m=0.1334 mm²/V*μs
y, mm

Fig. 1

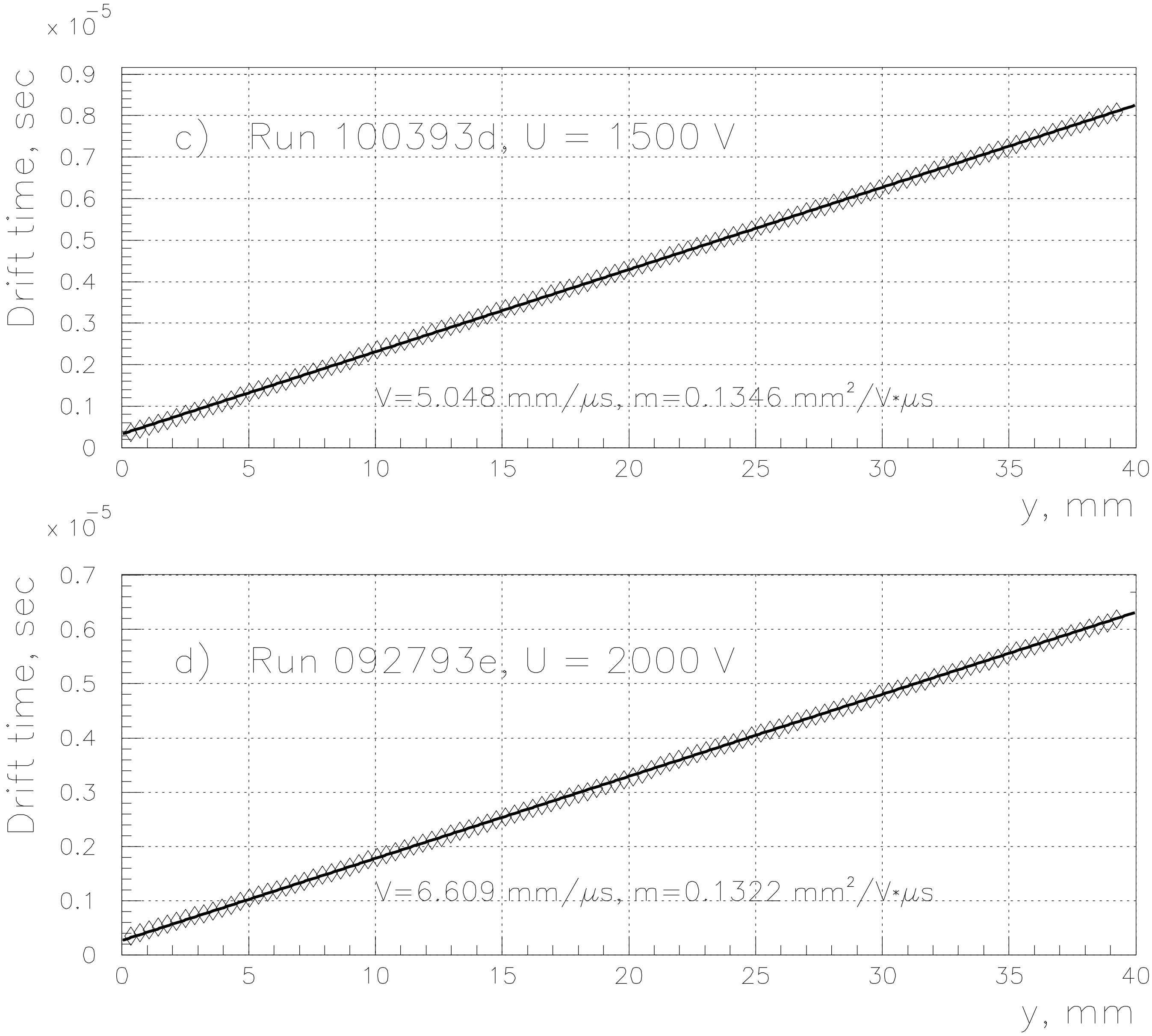
x 10^-5
Drift time, sec
c) Run 100393d, U = 1500 V
V=5.048 mm/μs, m=0.1346 mm²/V*μs
y, mm
x 10^-5
Drift time, sec
d) Run 092793e, U = 2000 V
V=6.609 mm/μs, m=0.1322 mm²/V*μs
y, mm

Fig. 1

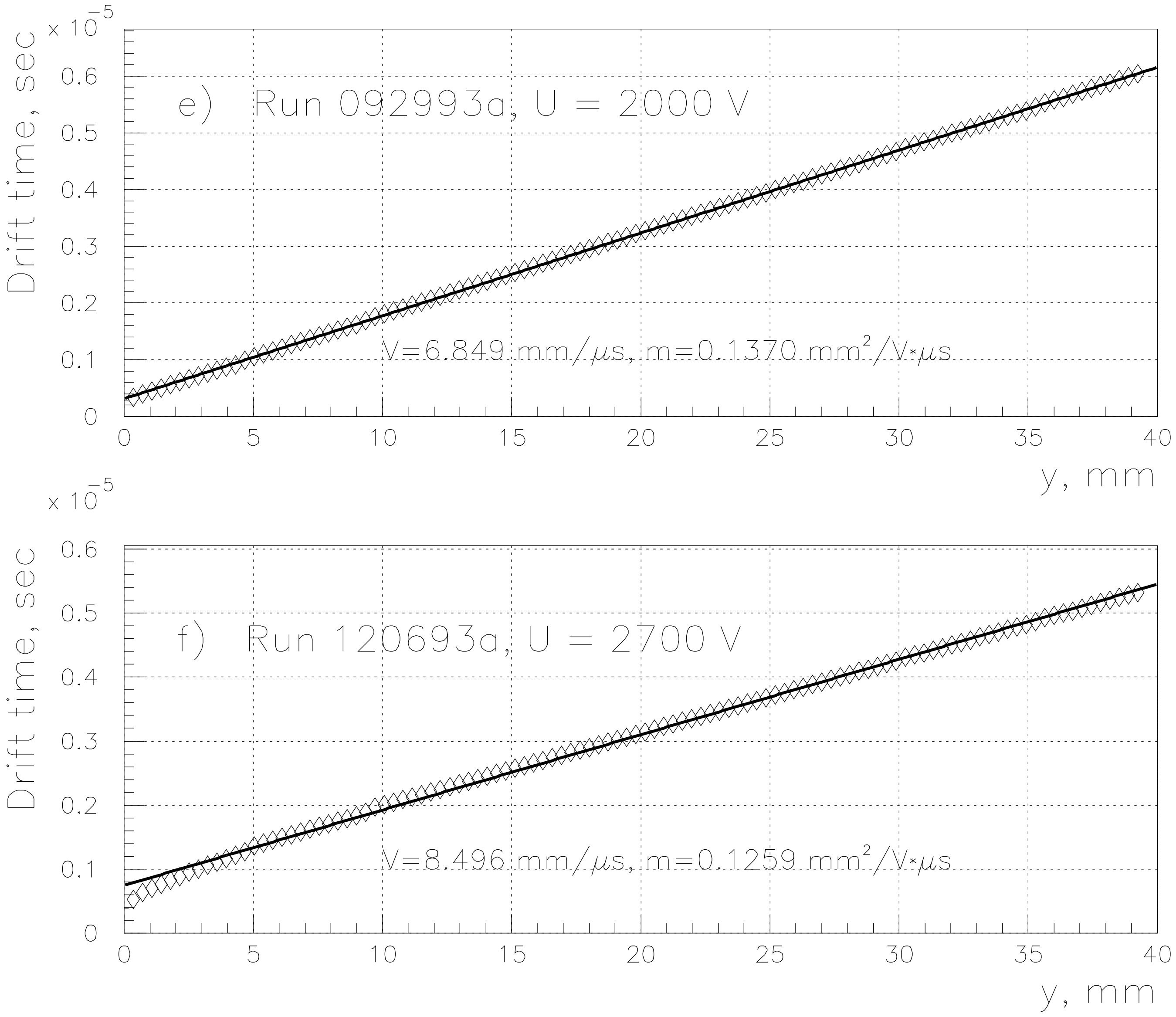
e) Run 092993a, U = 2000 V
V=6.849 mm/μs, m=0.1370 mm²/V∗μs
Drift time, sec
× 10⁻⁵
y, mm
f) Run 120693a, U = 2700 V
V=8.496 mm/μs, m=0.1259 mm²/V∗μs
Drift time, sec
× 10⁻⁵
y, mm

Fig. 1

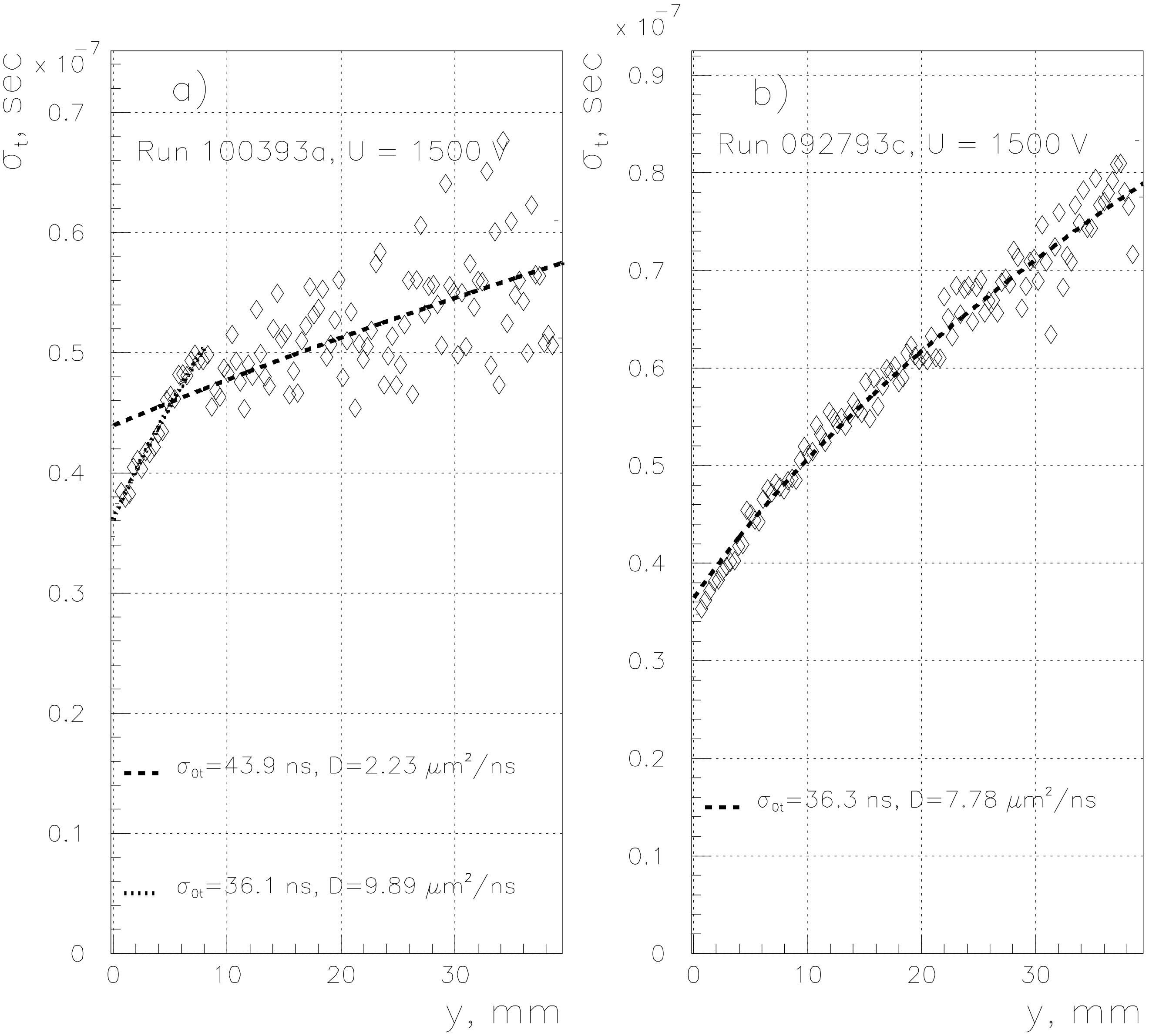

σ_t, sec
x 10^-7
a)
Run 100393a, U = 1500 V
σ_0t=43.9 ns, D=2.23 μm²/ns
σ_0t=36.1 ns, D=9.89 μm²/ns
y, mm
b)
Run 092793c, U = 1500 V
σ_0t=36.3 ns, D=7.78 μm²/ns
0
0.1
0.2
0.3
0.4
0.5
0.6
0.7
0.8
0.9
10
20
30

Fig. 2

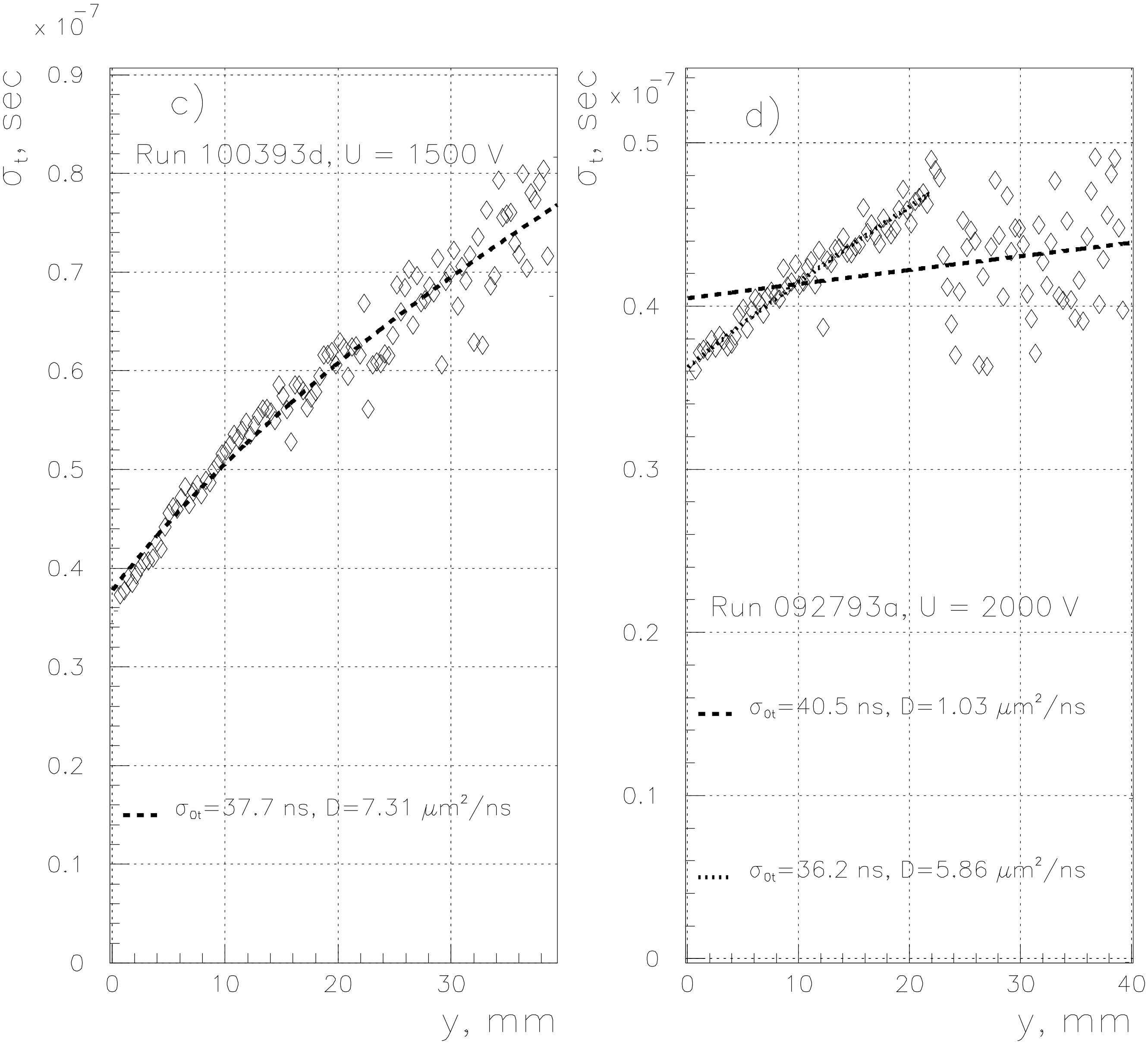

× 10^-7
σt, sec
c)
Run 100393d, U = 1500 V
σ0t=37.7 ns, D=7.31 μm²/ns
y, mm
d)
Run 092793a, U = 2000 V
σ0t=40.5 ns, D=1.03 μm²/ns
σ0t=36.2 ns, D=5.86 μm²/ns

Fig. 2

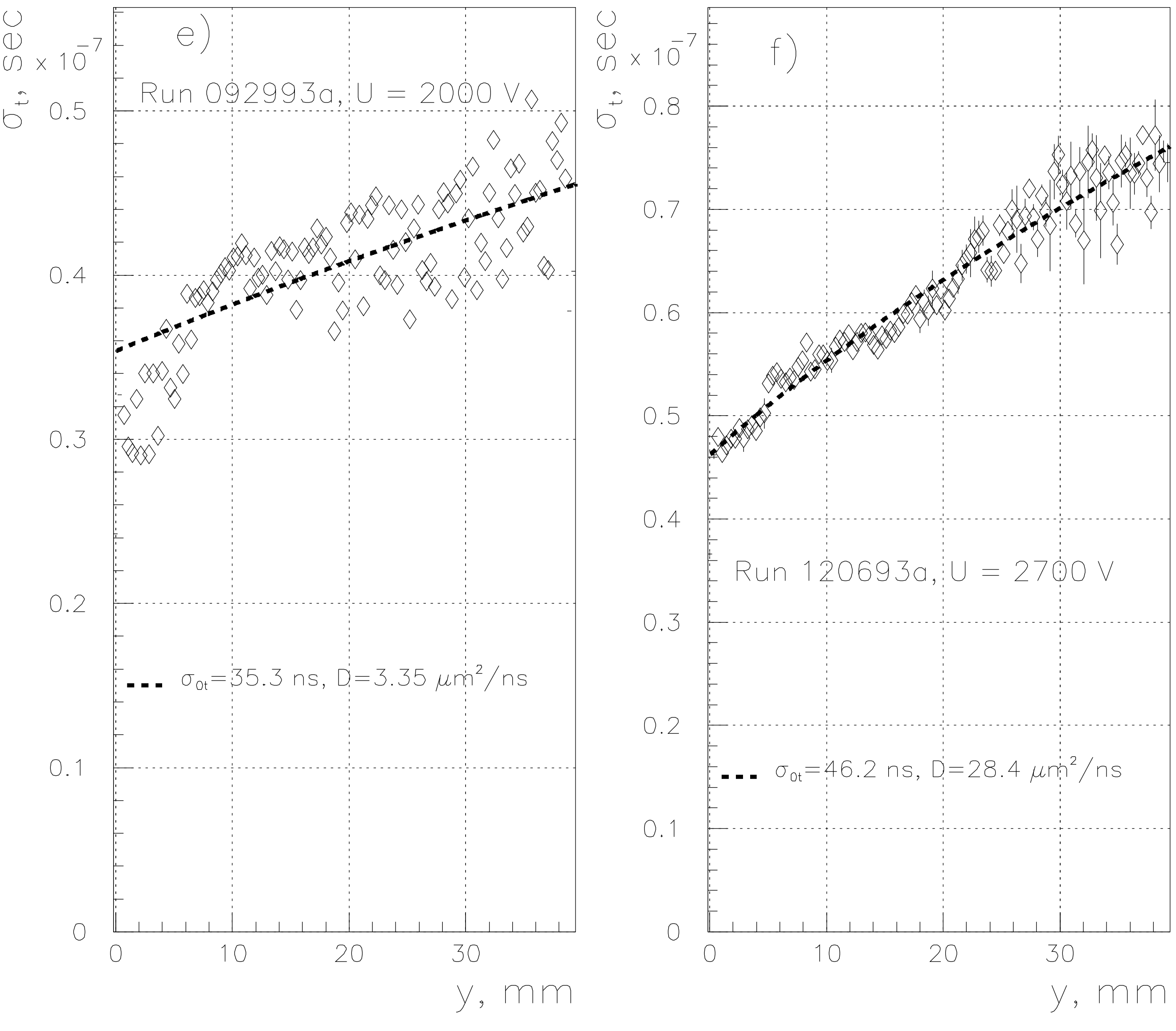

e)
Run 092993a, U = 2000 V
σ_{0t}=35.3 ns, D=3.35 μm^2/ns
σ_t, sec
x 10^{-7}
y, mm
f)
Run 120693a, U = 2700 V
σ_{0t}=46.2 ns, D=28.4 μm^2/ns

Fig. 2

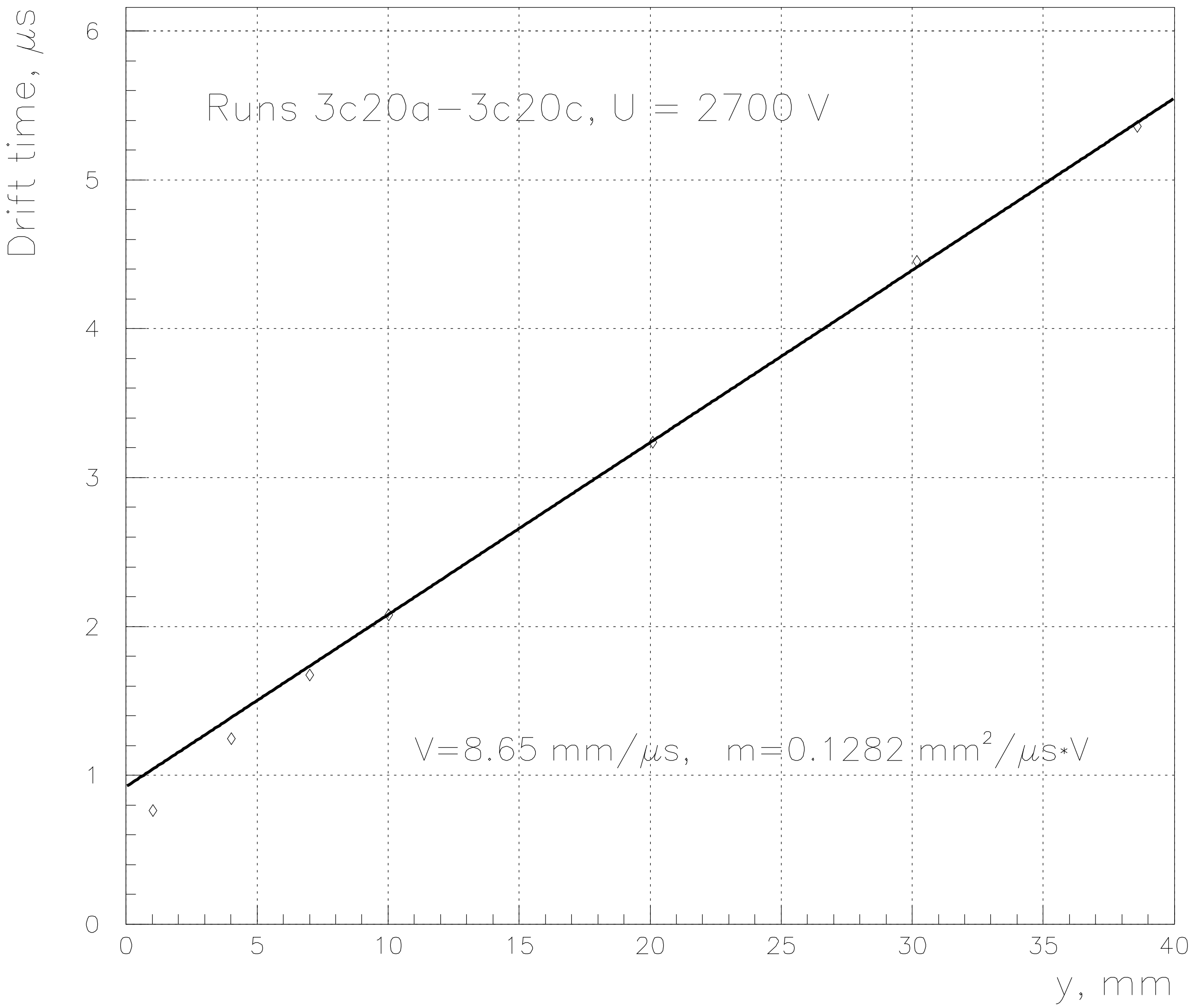
Drift time, μs
Runs 3c20a−3c20c, U = 2700 V
V=8.65 mm/μs, m=0.1282 mm²/μs*V
0
1
2
3
4
5
6
0
5
10
15
20
25
30
35
40
y, mm

Fig. 3

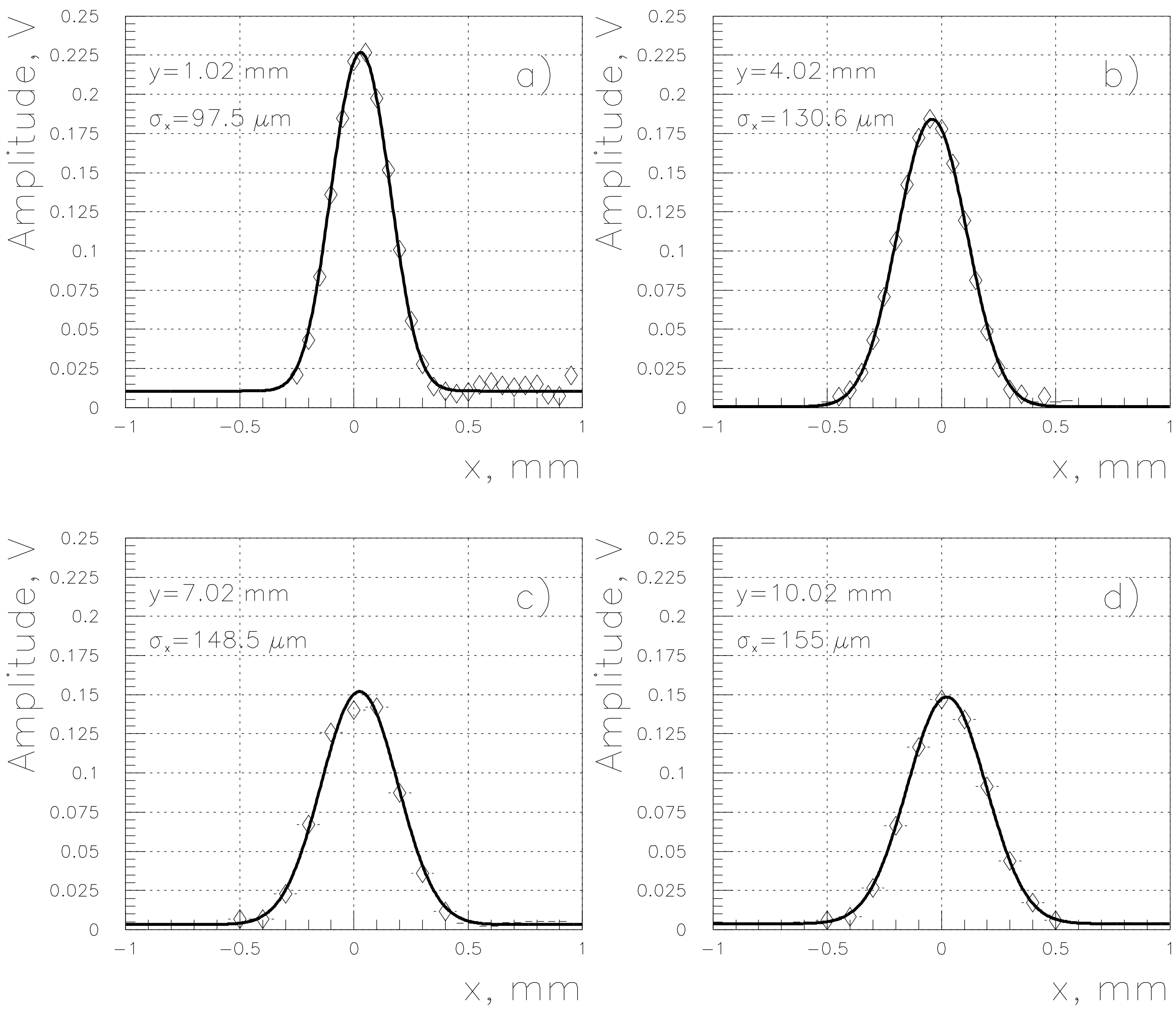

Amplitude, V
x, mm
y=1.02 mm
σ_x=97.5 μm
a)
y=4.02 mm
σ_x=130.6 μm
b)
y=7.02 mm
σ_x=148.5 μm
c)
y=10.02 mm
σ_x=155 μm
d)

Fig. 4

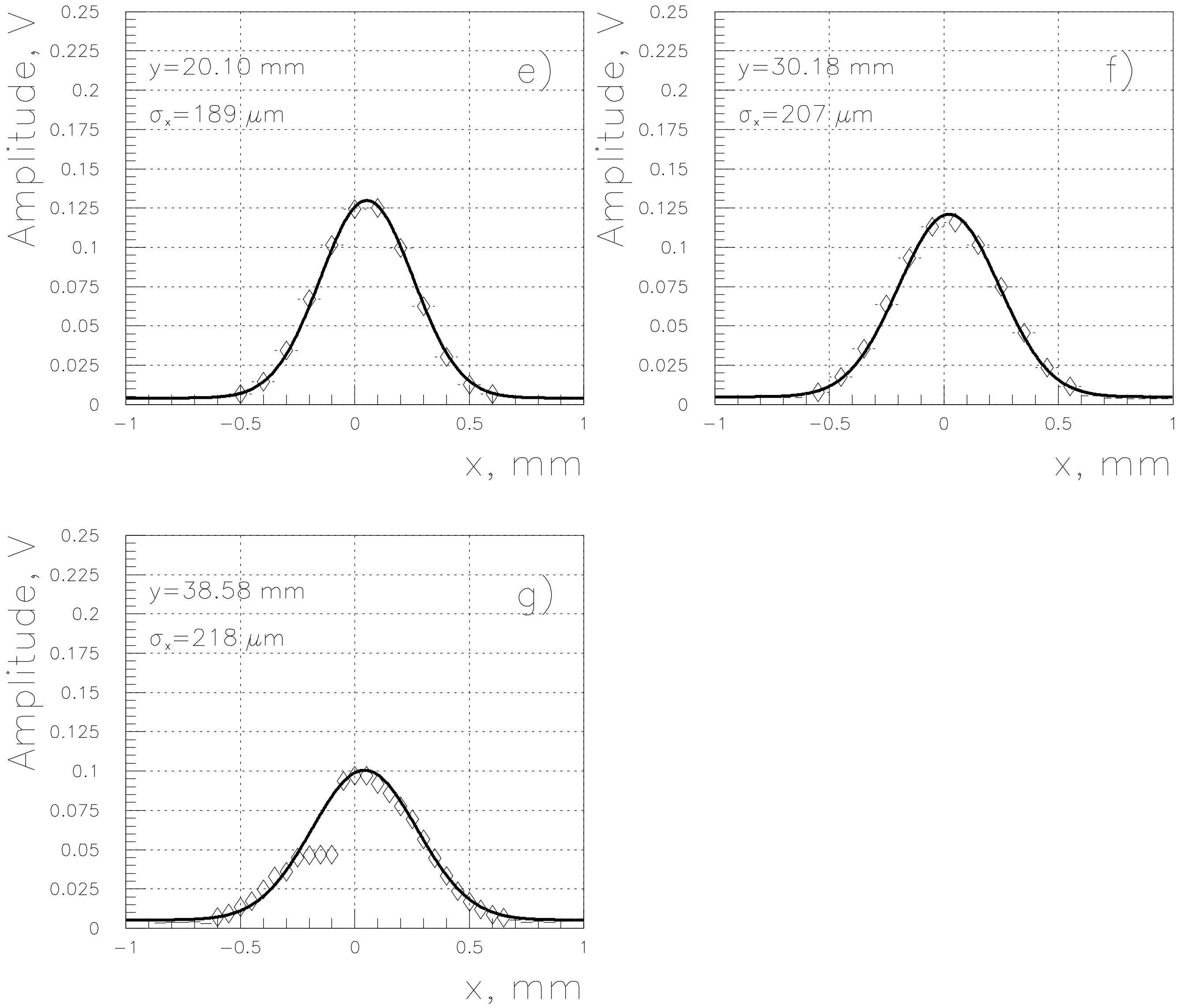

Amplitude, V
0.25
0.225
0.2
0.175
0.15
0.125
0.1
0.075
0.05
0.025
0
y=20.10 mm
σ_x=189 μm
e)
−1
−0.5
0
0.5
1
x, mm
y=30.18 mm
σ_x=207 μm
f)
y=38.58 mm
σ_x=218 μm
g)

Fig. 4

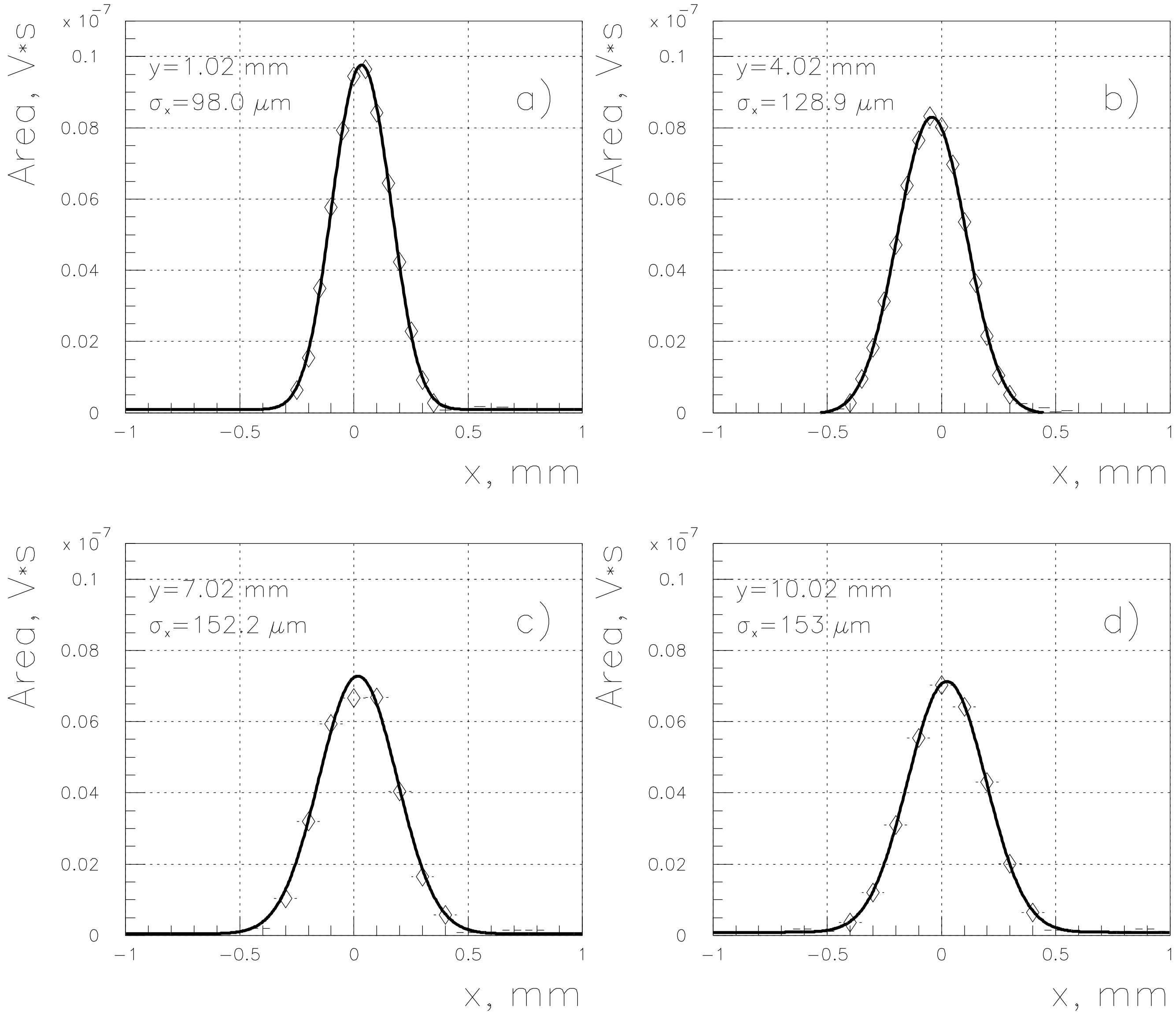

x 10^-7
Area, V*s
x, mm
y=1.02 mm
σx=98.0 μm
a)
y=4.02 mm
σx=128.9 μm
b)
y=7.02 mm
σx=152.2 μm
c)
y=10.02 mm
σx=153 μm
d)

Fig. 5

[p]

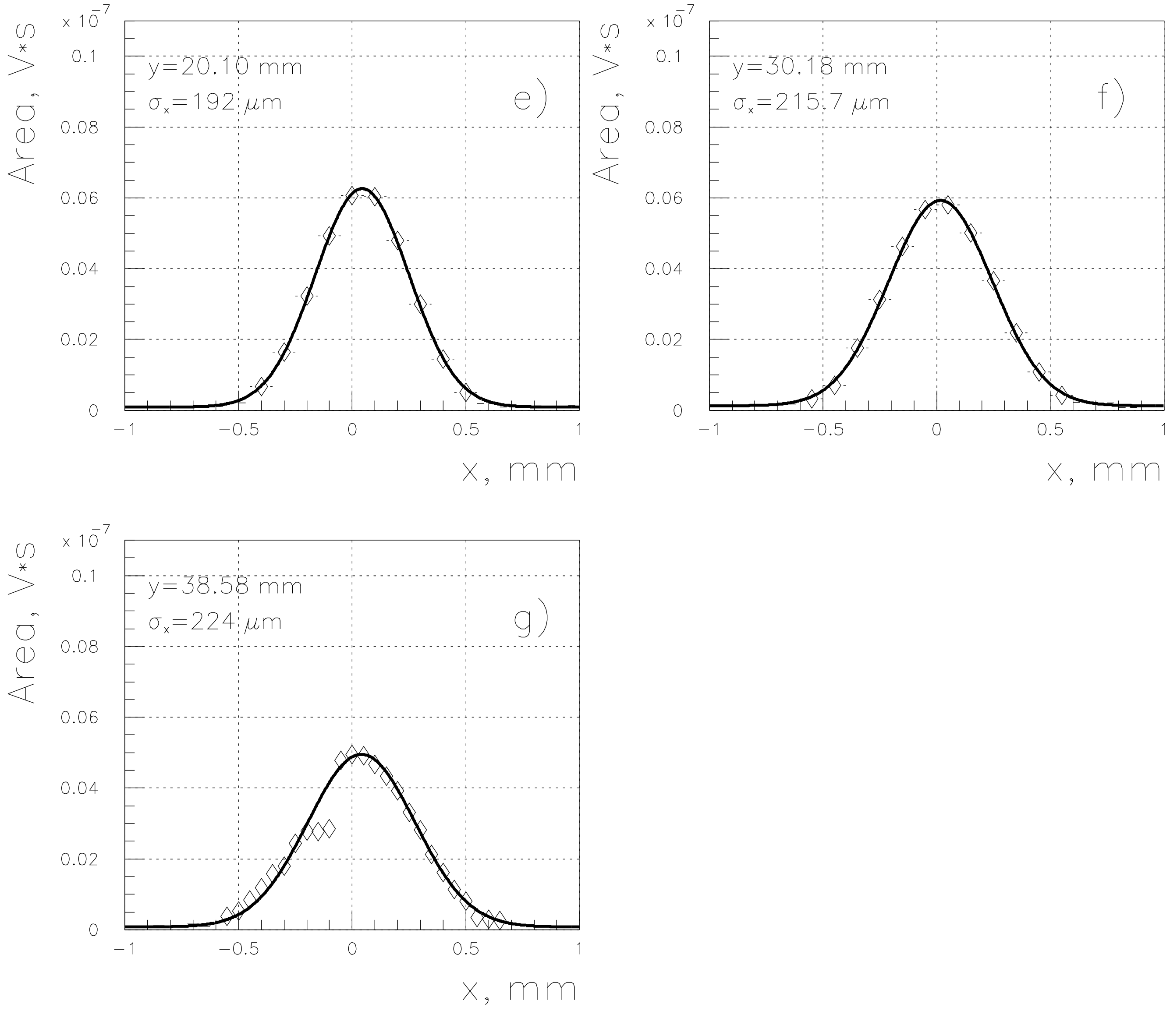
Area, V*s
x 10^{-7}
y=20.10 mm
σ_x=192 μm
e)
x, mm
y=30.18 mm
σ_x=215.7 μm
f)
y=38.58 mm
σ_x=224 μm
g)

Fig. 5

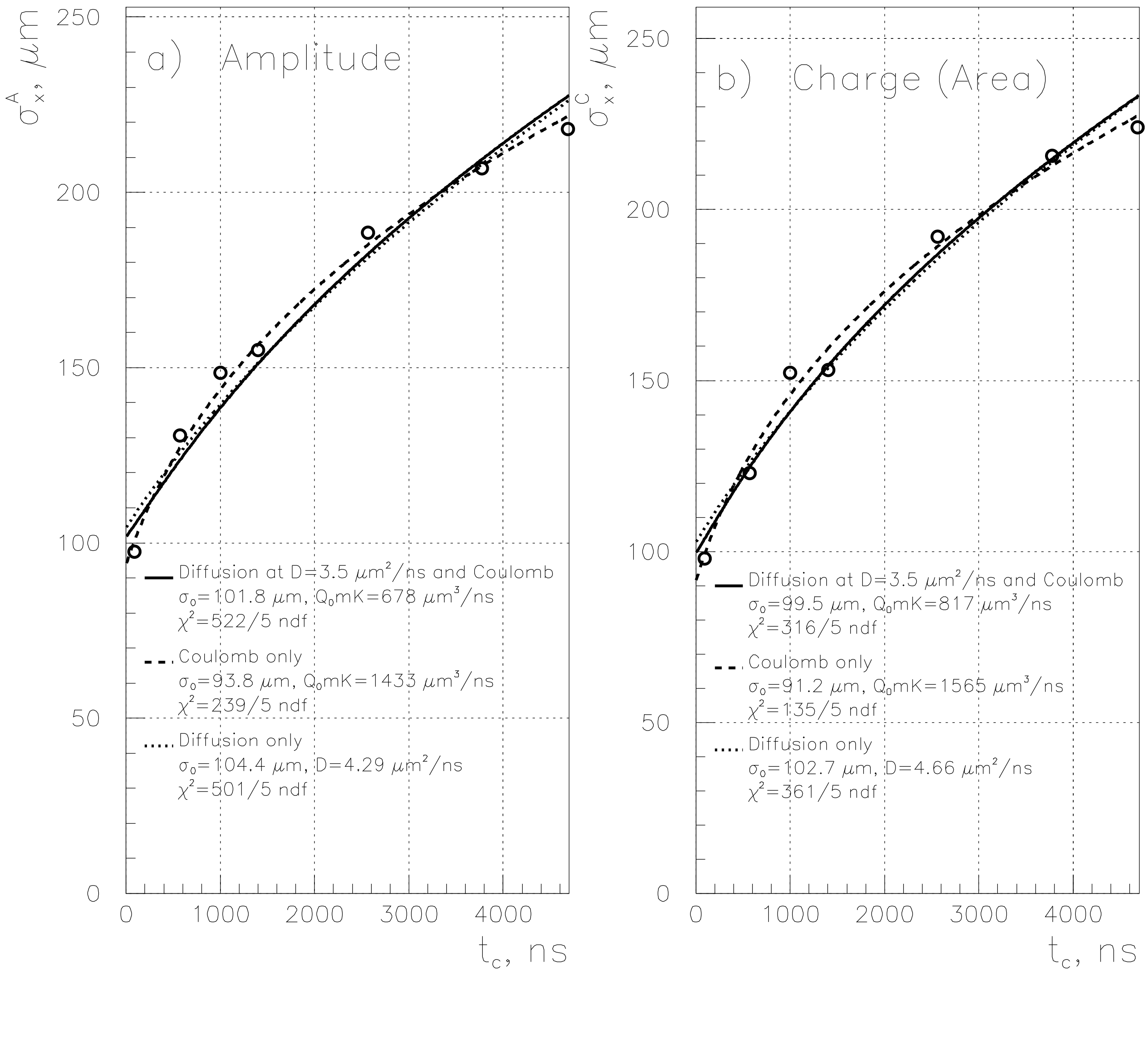
a) Amplitude
σ_x^A, μm
Diffusion at D=3.5 μm^2/ns and Coulomb
σ_0=101.8 μm, Q_0mK=678 μm^3/ns
χ^2=522/5 ndf
Coulomb only
σ_0=93.8 μm, Q_0mK=1433 μm^3/ns
χ^2=239/5 ndf
Diffusion only
σ_0=104.4 μm, D=4.29 μm^2/ns
χ^2=501/5 ndf
t_c, ns
b) Charge (Area)
σ_x^C, μm
Diffusion at D=3.5 μm^2/ns and Coulomb
σ_0=99.5 μm, Q_0mK=817 μm^3/ns
χ^2=316/5 ndf
Coulomb only
σ_0=91.2 μm, Q_0mK=1565 μm^3/ns
χ^2=135/5 ndf
Diffusion only
σ_0=102.7 μm, D=4.66 μm^2/ns
χ^2=361/5 ndf
t_c, ns

Fig. 6

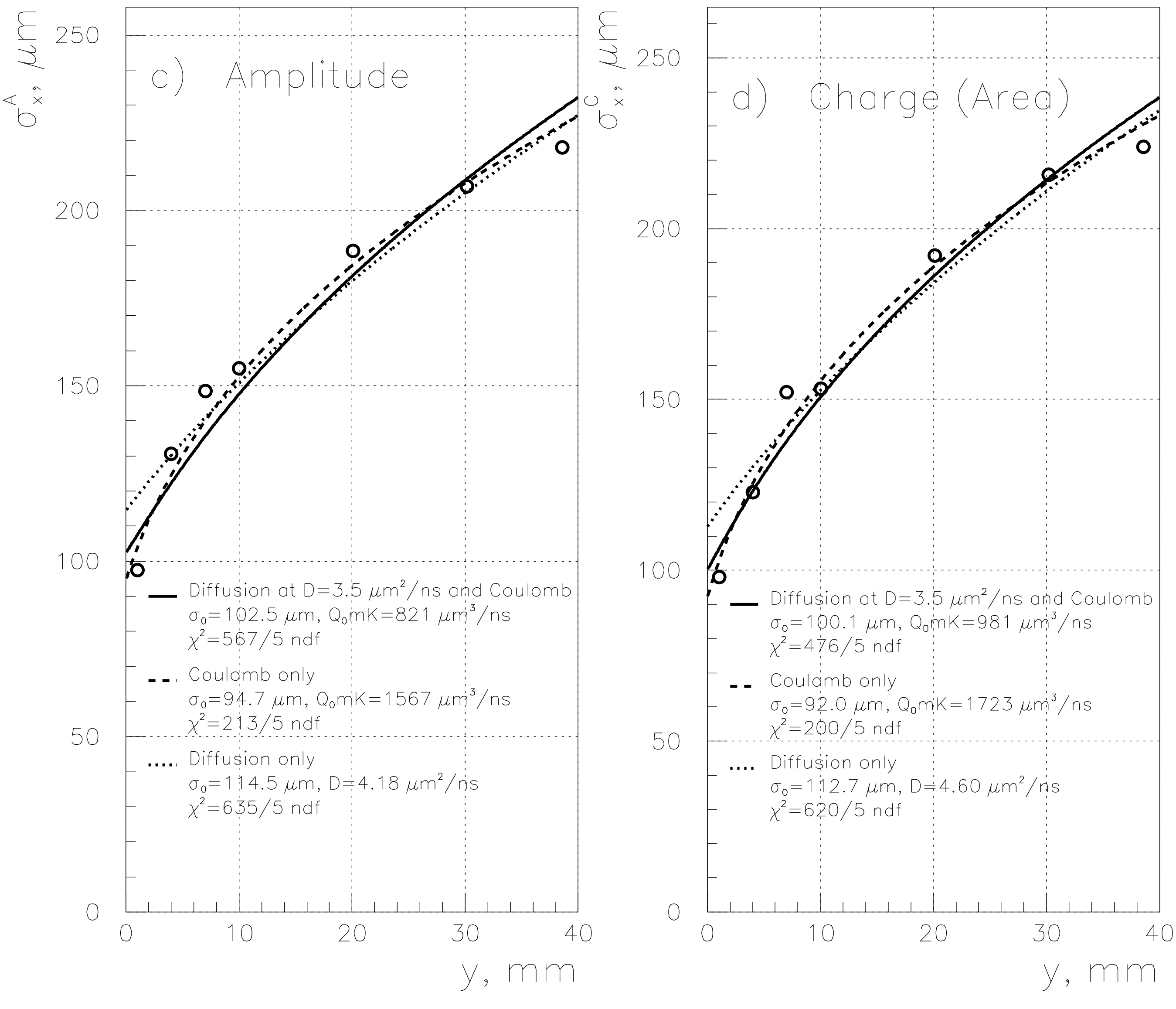

c) Amplitude
σ_x^A, μm
y, mm
Diffusion at D=3.5 μm^2/ns and Coulomb
σ_0=102.5 μm, $Q_0 mK$=821 μm^3/ns
χ^2=567/5 ndf
Coulomb only
σ_0=94.7 μm, $Q_0 mK$=1567 μm^3/ns
χ^2=213/5 ndf
Diffusion only
σ_0=114.5 μm, D=4.18 μm^2/ns
χ^2=635/5 ndf
d) Charge (Area)
σ_x^C, μm
y, mm
Diffusion at D=3.5 μm^2/ns and Coulomb
σ_0=100.1 μm, $Q_0 mK$=981 μm^3/ns
χ^2=476/5 ndf
Coulomb only
σ_0=92.0 μm, $Q_0 mK$=1723 μm^3/ns
χ^2=200/5 ndf
Diffusion only
σ_0=112.7 μm, D=4.60 μm^2/ns
χ^2=620/5 ndf

Fig. 6